Millijoule laser pulse delivery for spark ignition through kagome hollow-core fiber

B. Beaudou,[1] F. Gerôme,[1,*] Y. Y. Wang,[1,2] M. Alharbi,[1,2] T. D. Bradley,[1,2] G. Humbert,[1] J.-L. Auguste,[1] J.-M. Blondy,[1] and F. Benabid[1,2]

[1]GPPMM Group, Xlim-UMR 7252 Université de Limoges/CNRS, 123 Avenue Albert Thomas, 87060 Limoges Cedex, France

[2]Gas-Phase Photonic Materials Group, CPPM, University of Bath, Claverton Down, Bath, BA2 7AY, UK

*Corresponding author: gerome@xlim.fr

Received January 18, 2012; revised February 29, 2012; accepted March 6, 2012;
posted March 6, 2012 (Doc. ID 161518); published April 23, 2012

We report on power handling oriented design of kagome lattice hollow-core fiber and demonstrate through it for the first time nanosecond laser pulses induced spark ignition in a friendly manner. Two different core designs and transmission bands are investigated and evaluated. The energy threshold damage was measured to be in excess of the 10 mJ level and the output power density is approaching the TW/cm^2 after focusing; demonstrating the outstanding ability of such fiber for high power delivery. © 2012 Optical Society of America

OCIS codes: 060.5295, 140.3440.

Laser-induced spark ignition has proved to offer several significant advantages over the conventional spark-ignition system based on electrical breakdown. Among these advantages we count higher efficiency to ignite leaner mixtures, reduction of erosion effects, selective chemistry, increase of engine efficiency, or shorter combustion time to mention a few [1]. This in turn triggered an ongoing research in laser spark ignition through optical fiber for its considerable and broad potential in providing flexible laser beam delivery. However, the low material's laser induced damage threshold (LIDT) of optical fiber has hindered its successful implementation. Indeed, the typical LIDT of the silica glass, the standard material for conventional optical fiber, is much lower than the minimum power density required for sparking triggering in air or gas mixtures (typically several TW/cm^2).

Recalling that for efficient spark ignition, one must meet several requirements. Firstly, a high level of power density, which in turn calls for a tight laser beam focusing configuration. Secondly, for practical application a flexible delivery of the laser beam is necessary. Finally, for efficient laser-induce spark ignition, the laser beam should exhibit a M^2 close to unity. All these restrictions push researchers to investigate the use of hollow-core capillary fiber because of its air-guidance properties. However the higher optical transmission and sensitivity to bend were a hindrance [2].

The advent of hollow-core photonic crystal fiber (HC-PCF) stimulated a renewed interest in fiber based high power laser delivery. Previous investigations demonstrated the ability of photonic bandgap (PBG) guiding HC-PCF in delivering high energy laser pulses in both the nanosecond [3] and femtosecond [4] pulse duration regimes. Unfortunately, the relatively small core diameter PBG guiding HC-PCF (typically the fiber diameter D_C is in the range 5–10 μm) and the strong power overlap between the hollow-core and the silica core-surround limited the energies to less than 1 mJ for nanosecond laser pulses [3] and to less than 1 μJ for sub-picosecond pulses [4] that one could couple into these fibers. In parallel to the PBG guiding HC-PCF, we count a second class of HC-PCF coined kagome-like HC-PCF [5]. Owing to its intrinsic guidance mechanism, this fiber proved to exhibit much lower power overlap with the silica part of the fiber structure [6], which is confirmed with the first demonstration of high harmonic generation [7]. Moreover, the combination of this laser power handling capabilities and the low numerical aperture of the kagome HC-PCF makes this type of HC-PCF an ideal system for laser-induced spark ignition [2].

Two kagome-like HC-PCFs were fabricated and investigated with the aim to optimize the guidance of high energy laser pulses around 1064 nm. The first one is a single-cell core [8] with a cladding consisting of two rings of kagome lattice with a pitch of 28 μm and strut thickness of 640 nm [see inset of Fig. 1(a)]. The second fiber is a 7-cell core with hypocycloid shape and three rings of kagome lattice cladding [9] with a pitch of 20 μm and strut thickness of 320 nm [see inset of Fig. 1(b)]. Figures 1(a) and 1(b) show the transmission and loss spectra for the two fibers. The single-cell HC-PCF exhibits two main transmission windows with a typical loss figure of around 1 dB/m. The first spans from ~700 to 1300 nm with edges qualitatively corresponding to the wavelengths of the second and first order of the transverse resonance [6]:

$$\lambda_m \cong \frac{2}{m} t \sqrt{n_{\mathrm{glass}}^2 - 1}. \tag{1}$$

Here t is the silica-strut thickness, n_{glass} is the index of the silica, and m is the order integer. The second transmission window spans from ~450 to 700 nm. The second HC-PCF (figure 1(b)) exhibits a much lower loss (typically ~250 dB/km) over broader range (from ~800 to >1750 nm). This is explained by the thinner struts and secondly by the guidance mechanism [10–12]. Indeed, for the main transmission window of this fiber, the optical guidance is dominated by inhibited coupling mechanism, while for the other higher order transmission bands the confining power of the inhibited coupling diminishes [9], and consequently the guidance is strongly influenced by the anti-resonant attribute of the thin silica core surround [6,8,9].

Here the physical and optical characteristics (e.g. strut thickness, pitch and optical loss) were chosen to provide

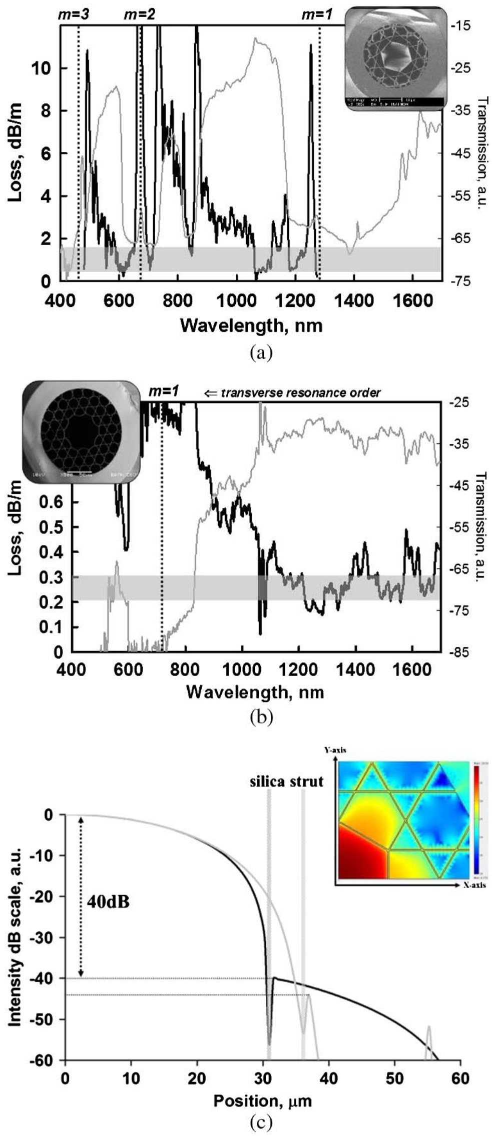

Fig. 1. (Color online) (a) Loss and transmission spectra measured for a kagome-like fiber designing to operate on the first high-order band (thickness of the core surround of 640 nm) (Media 1) and (b) on the fundamental band (thickness of the core surround of 320 nm) at 1064 nm (Media 2). In inset the SEM micrograph of the fabricated fibers and the transverse resonance order are added. (c) Theoretical intensity of the field distribution at 1064 nm for a typical fundamental mode of a kagome-like fiber (black, X axis; gray, Y axis) plotted in dB scale (Media 3).

comparative data on the optimum fiber design for high power flexible delivery for spark ignition. In particular, a choice must be made on the ideal strut thickness to have a trade-off between the transmission performance and the power overlap with the silica struts, as they chiefly determine the performance of the fiber for spark ignition.

Indeed, the theoretical maximum energy one could couple into the fiber can be written as $E_{\max} \sim (\mathrm{LIDT})(A_{\mathrm{ring}}/\eta)$, where LIDT is the guiding material laser intensity damage threshold of the silica core-surround, A_{ring} is the area of the silica core-surround and η is the theoretical optical power overlap ratio between the hollow-core and silica core-surround [13]. The expression clearly shows opposing trends of having thicker core surround to maximize the power handling and thinner struts to decrease the overlap for the thickness range considered here and improve the guidance. The LIDT for bulk silica is equal to 120 J/cm^2 for 9 ns pulses at 1064 nm. Figure 1(c) shows the calculated mode profile along two axes of the HE_{11} core mode for the single-cell fiber at $\lambda = 1064$ nm. The figure clearly illustrates the little overlap with silica (more than 40 dB extinction ratio between the intensity in the air core and the silica core-surround), corresponding to η of less than ~0.05%. The figure is of the same order as for the second HC-PCF and is lower by more than one order of magnitude compared to the PBG HC-PCF. The above-mentioned fibers are then inserted into the experimental setup shown in Fig. 2(a). The setup comprises a Nd:YAG 9 ns pulsed laser which can deliver 10 mJ at 1064 nm with a repetition rate of 5 Hz and a TEM_{00} mode profile. A Glan polarizer is then used to control the incident energy and dielectric high power mirrors are added to adjust the angle of the incident beam. The focused spot is launched into the HC-PCF under test using 53 mm effective focal length lens. The fiber length was 60 cm for the single cell fiber and ~1 m for the hypocycloid. The fiber is first flushed with Neon to remove any trapped dust inside the fiber core. The output is then refocused with an 8 mm aspheric

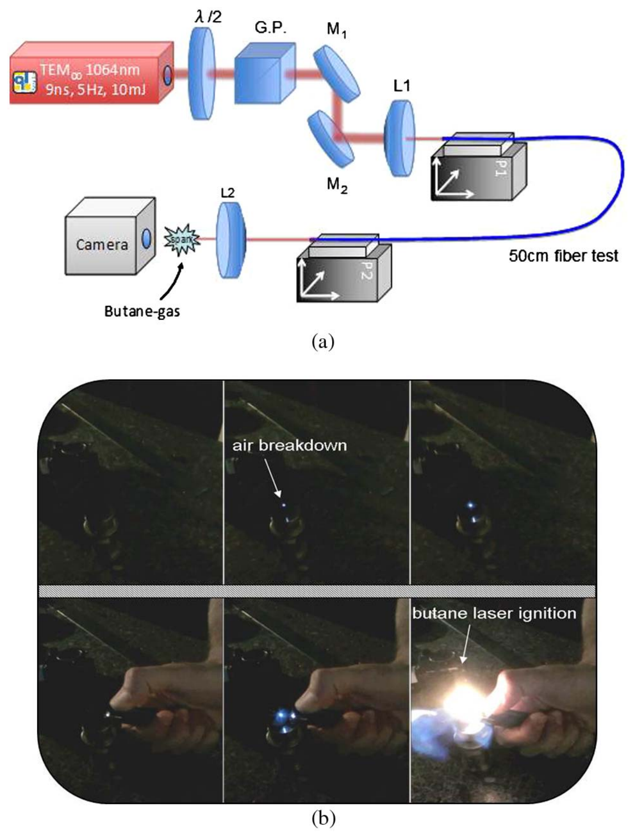

Fig. 2. (Color online) (a) Experimental setup (Media 4). $\lambda/2$, half-wave plate at 1064 nm; G.P., Glan polarizer; M, mirrors; L, lenses. (b) Air breakdown demonstration (power density at the focal point approaching TW/cm^2) at the fiber output after focusing (Media 5). At the bottom, pictures show the spark ignition induced.

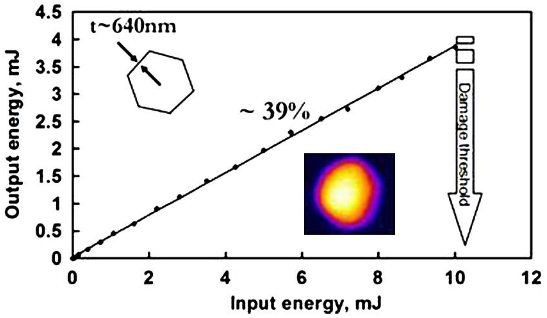

(a)

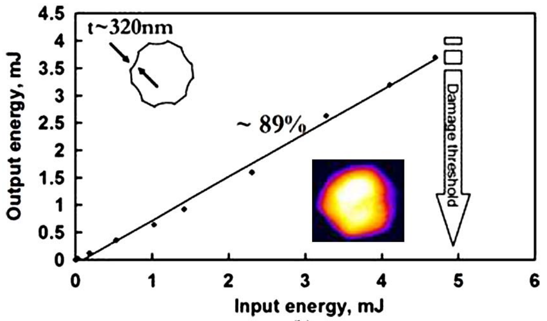

(b)

Fig. 3. (Color online) (a) Output energy versus input energy for a kagome-like fiber with a silica core surround thickness of 640 nm (Media 6) and (b) 320 nm (Media 7). The coupling efficiency and the damage threshold are indicated on the graphs. Insets: Near-field intensity patterns recorded at the fiber output.

lens to achieve sparking. Figure 2(b) shows the air breakdown induced by the focused beam (top frames), when a laser pulse of 2 mJ or more is delivered by the HC-PCF.

As a proof-of-concept of the capabilities of the fiber delivered laser beam for spark ignition, a jet of butane from a lighter is set near the focal position of the focusing lens. The bottom frame of Fig. 2(b) shows three frames illustrating the sequence of the spark ignition. Frame one corresponds to the release of the butane in the absence of the pulse. Frame two and three capture the ignition process by laser pulses of energy of 2 mJ or more. For a definitive implementation of our scheme to engine based applications further investigation of butane/air mixture laser ignition with different ratio and pressure is required. The air breakdown and the ignition were observed with both fibers to occur at the same energy level. However, the two fibers exhibit different characteristic regarding the transmission performance and the energy damage threshold. Figure 3 illustrates this difference. It shows the output energy in function of the input one for the single-core fiber [Fig. 3(a)] and for the hypocycloid one [Fig. 3(b)], respectively.

The maximum output energy of 4 mJ level was achieved for both fibers, but we could see discrepancies in coupling efficiency. The energy coupled in the core is nearly optimal and reaches 89% of the incoming power for the hypocycloid core HC-PCF, while only 39% is transmitted for the single-core fiber. The lack of available data on thin silica LIDT, along with and the presence of contamination (dust) the imperfect coupling conditions and imperfections at the fiber input end are responsible to the discrepancy between the theoretical maximum energy and the experimentally achieved in this paper. The imaging of the reconstructed near-field and the far-field of the fiber outputs (see insets of Fig. 3) indicate a near-Gaussian beam behavior, thus making HC-PCF an excellent means for a flexible delivery tool for laser-induced spark ignition. The reached energy level is increased by nearly an order of magnitude compared to previous work on PBG guiding HC-PCF [2,3] and can be brought closer to theoretical limit by improving the setup and the end facet preparation.

In conclusion, high-transmitted energy level and good spatial quality allow us to tightly refocus the outgoing beam and overtake the air ionization breakdown threshold. This is, to the best of our knowledge, the first demonstration of HC-PCF delivery for spark ignition application.

The authors wish to thank G. Gaborel from Meggitt for his help and fruitful discussions and Quantel for the loan of the laser. This research was supported and funded by the French Army through grant 2009-34-0037 and the EPSRC KTA program.

References

1. J. X. Ma, D. R. Alexander, and D. E. Poulain, Combust. Flame **112**, 492 (1998).
2. S. Joshi, A. P. Yalin, and A. Galvanauskas, Appl. Opt. **46**, 4057 (2007).
3. J. Shephard, J. Jones, D. Hand, G. Bouwmans, J. Knight, P. Russell, and B. Mangan, Opt. Express **12**, 717 (2004).
4. D. G. Ouzounov, F. R. Ahmad, D. Müller, N. Venkataraman, M. T. Gallagher, M. G. Thomas, J. Silcox, K. W. Koch, and A. L. Gaeta, Science **301**, 1702 (2003).
5. F. Benabid and J. P. Roberts, J. Mod. Opt. **58**, 87 (2011).
6. F. Couny, F. Benabid, P. J. Roberts, P. S. Light, and M. G. Raymer, Science **318**, 1118 (2007).
7. O. H. Heckl, C. R. E. Baer, C. Kränkel, S. V. Marchese, F. Schapper, M. Holler, T. Südmeyer, J. S. Robinson, J. W. G. Tisch, F. Couny, P. Light, F. Benabid, and U. Keller, Appl. Phys. B: Lasers Opt. **97**, 369 (2009).
8. F. Gérôme, R. Jamier, J. L. Auguste, G. Humbert, and J. M. Blondy, Opt. Lett. **35**, 1157 (2010).
9. Y. Y. Wang, N. V. Wheeler, F. Couny, P. J. Roberts, and F. Benabid, Opt. Lett. **36**, 669 (2011).
10. G. J. Pearce, G. S. Wiederhecker, C. G. Poulton, S. Burger, and P. Russell, Opt. Express **15**, 12680 (2007).
11. L. Chen, G. J. Pearce, T. Birks, and D. Bird, Opt. Express **19**, 6945 (2011).
12. L. Chen and D. Bird, Opt. Express **19**, 6957 (2011).
13. P. J. Roberts, D. P. Williams, B. Mangan, H. Sabert, F. Couny, W. J. Wadsworth, T. Birks, J. Knight, and P. Russell, Opt. Express **13**, 8277 (2005).